Electronic Supplementary Material (ESI) for Physical Chemistry Chemical Physics.

Ligand Influence on the Electronic Spectra of Monocationic Copper-Bipyridine Complexes

Supplementary Information

Shuǎng Xú[1], Samer Gozem,[2] Anna I. Krylov,[2] Casey R. Christopher[3] and J. Mathias Weber[3,]*

[1]JILA and Department of Physics, University of Colorado, Boulder, CO 80309-0440, USA

[2]Department of Chemistry, University of Southern California,

Los Angeles, CA 90089-0482, USA

[3]JILA and Department of Chemistry and Biochemistry, University of Colorado,

Boulder, CO 80309-0440, USA

Table of Contents

Detailed description of the experimental setup

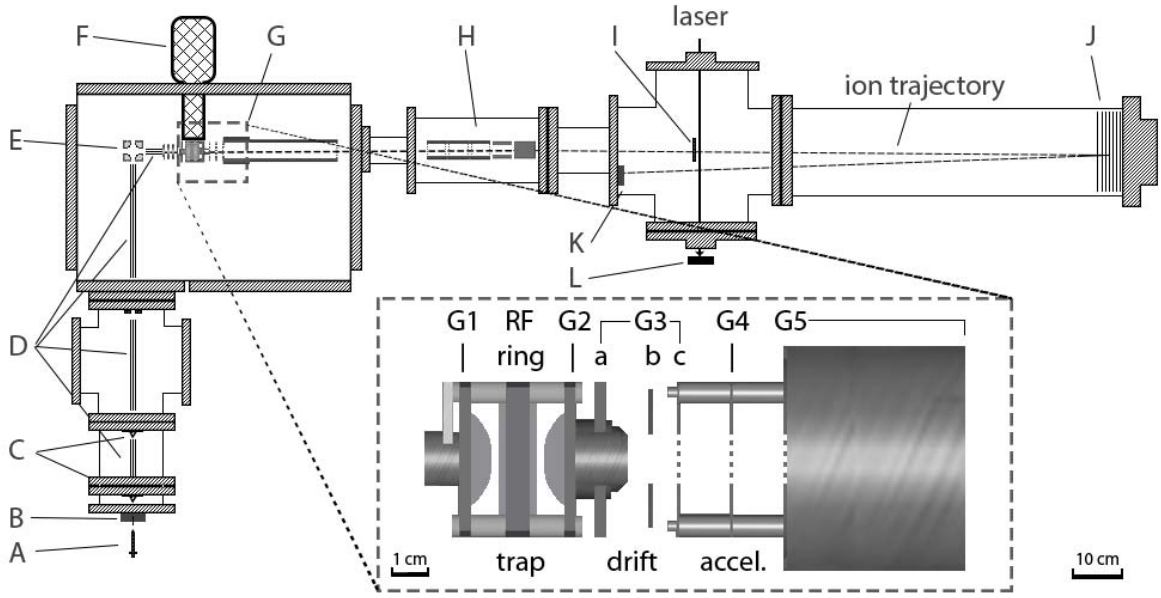

Figure S1. Schematic of the experimental apparatus. A: electrospray needle; B: desolvation capillary; C: skimmers; D: octupole ion guides; E: quadrupole bender; F: helium cryostat; G: quadrupole ion trap and acceleration unit (inset shows details, see text); H: ion lens and deflectors; I: mass gate; J: reflectron; K: microchannel plate detector; L: laser power meter.

1. Electrospray ionization source

Electrospray ionization is performed using a commercial needle assembly (Analytica of Branford). Inside an outer spraying needle is silica capillary tubing (75 μm ID, 193 μm OD, Polymicro Technologies) that extends 1-2 mm out of the needle tip. Dry N_2 (30-40 psi) is fed through the outer needle, serving as the nebulizing gas around the tip. The needle assembly is mounted on a 3-axis translation stage to aid positioning relative to the desolvation capillary.

The desolvation capillary is made of stainless steel, and has an ID of 0.5 mm and a length of 58.4 mm. It is housed in a heated copper cylinder whose temperature is monitored and controlled using a type K thermocouple, a cartridge heater and a temperature controller (Omega CN9000A).

In the present work, the source solution is an equal volume mixture of 5 mM solutions of copper(II) salt and 2,2'-bipyridine in a 1:4 mixture of distilled water and methanol (HPLC grade, EMD Millipore). Copper(II) nitrate hydrate (99.999%, trace metals basis, for L = N_2 and H_2O) and 2,2'-bipyridine (ReagentPlus grade, ≥99%) were purchased from Sigma-Aldrich, while copper(II) chloride dehydrate (99+%, ACS grade, for L = Cl) was purchased from Alfa Aesar. All chemicals were used without further purification. The solution is pumped to the ESI needle at 25 µL/h by a syringe pump (New Era, model NE-1000). The spraying needle is held at +3 kV and the desolvation capillary is heated to 70 °C in order to achieve optimal ion intensity.

2. Ion guides and pre-trap ion optics

Ions exiting the desolvation capillary into the first differential pumping stage (ca. 1 mbar, pumped by 65 m^3/h rotary vane pump, Leybold Trivac D65 B) are focused by a tube lens (3.2 mm ID, 3 mm long) into a skimmer (1.5 mm diameter, ca. 2 mm distance from the tube lens) before entering a series of three home-built octupole ion guides (ID 9 mm, rod diameter 3 mm). The first (length 139 mm) guides the ions through the second differential pumping stage (ca. 0.2 mbar, pumped by 65 m^3/h rotary vane pump, Leybold Trivac D65 B) and into a second skimmer (1.5 mm diameter). The next octupole guide (length 313 mm) and differential pumping stage (ca. 10^{-4} mbar, pumped by a 685 L/s turbomolecular pump, Pfeiffer HiPace 700) end at a 10 mm orifice, leading into the chamber that houses the ion trap and the TOF acceleration unit.

All ion guides are driven by home-built radiofrequency power supplies (10 MHz, 300-750 V peak-to-peak) which can be biased by DC voltages. Likewise, the desolvation capillary, both skimmers and the orifice behind the second ion guide are biased by DC voltages.

In the TOF acceleration chamber (pumped by a 1100 L/s turbomolecular pump, Leybold Turbovac 1000 C), the ions are guided by a third octupole (length 304 mm) into a home built quadrupole bender, then guided by a short (length 39 mm) fourth octupole into an Einzel lens and focused into a 3-dimensional Paul trap.

3. Cryogenic ion trap

We use a three-dimensional Paul trap in this setup (Jordan TOF Products). The ring electrode is driven with 1 MHz radio frequency (0-4 kV peak-to-peak voltage) using the power supply provided by the manufacturer. Typical values for DC bias voltage on this electrode are up to ±30 V. The two end cap electrodes (G1 and G2) and an electrode outside the trap (G3-a) are used to apply electric fields suitable for loading and ejecting the ions from the trap, using pulsed home-built power supplies. During the loading period the field decelerates the ions, while during the ejecting period it propels the ions to the next stage. The magnitude of the field is ~30 V/cm for loading and ~200 V/cm for ejecting. One complete cycle of loading and ejecting takes 50 ms in this experiment, with 48.5 ms devoted to loading. Buffer gas (He or He seeded with small amounts of other gases) is introduced into the trap at the beginning of the loading period. It is pulsed through a general valve (Parker General Valve Series 99), keeping the average ambient pressure in the chamber of the order of 10^{-6} mbar.

The trap is mounted on the cold finger of a closed cycle helium cryostat (Sumitomo F-70L) with a 1-mm-thick sapphire substrate for electrical insulation. The cold finger can be cooled to 3.5 K and its temperature is measured with a Si diode (LakeShore 336 temperature controller). The trap temperature itself is measured with a second Si diode. The entire trap is enclosed in a copper housing directly contacting the radiation shield of the cryostat kept at about 60 K. The buffer gas

valve is mounted on the copper housing and the upstream tubing is also attached to the shield for precooling purpose. In this work the buffer gas used was He (5.0, Airgas). The temperature of the trap in the present work was 50 K, with the exception of the N_2 complexes, where the temperature was kept at 70 K.

4. Mass spectrometer

Following the trap is a set (G3) of three equipotential electrodes between the trap and the acceleration region of the Wiley-McLaren RETOF. The first (G3-a) is a short tube (15.2 mm long, 11.5 mm ID) that is integrated with the exit end cap of the trap (G2), as previously mentioned. The second (G3-b) is a thin (0.64 mm) electrode with a 12.7 mm orifice and is mounted on the heat shield. The third (G3-c) sits outside the heat shield and also serves as the first electrode of the accelerator unit of the Wiley-McLaren RETOF. The accelerator unit consists of G3-c followed by other two electrodes (G4 and G5), all spaced by 14 mm. G3-c and G4 have the same dimensions as G3-b, but their apertures are covered by a wire mesh (90% transmission); G5 is similar to G4, but attached to a tube (265 mm long, 44.5 mm ID). It takes a few microseconds for the ejected ion packet to drift through G3 and reach the acceleration region. Because this drift time depends on the mass-to-charge ratio of ions, an ion packet containing various species will be elongated along the moving direction. As a result, once a certain delay is set, only part of the packet can be accelerated efficiently and thus can be observed on the mass spectrum. Timing and voltages are critical for optimal mass resolution (up to $m/\Delta m = 1200$ were observed in the present experiment).

Alternatively, ions can be directly accelerated using the two end caps of the trap (G1 and G2) and electrode G3-a. In this case, full mass spectra can be measured, and mass resolutions up to

$m/\Delta m = 2200$ are possible, but the locally high density of buffer gas inside the trap can lead to strong collisional heating during acceleration.

When the ion packet is accelerated, electrodes G4 and G5 are pulsed to -325 V and -3800 V, respectively (cation mode). The high voltages are held until the ion packet enters the tube part of G5, then all electrodes are switched to ground. The acceleration voltages are carefully chosen to ensure an optimal space focus in the laser irradiation region.

Following acceleration the ion packet enters a differential pumping stage (ca 10^{-7} mbar, pumped by a 230 L/s turbomolecular pump, Pfeiffer TMU261) containing an Einzel lens consisting of three cylindrical electrodes (45.7 mm long, 30.5 mm ID) and a set of electrostatic deflectors for beam steering. Each deflector consists of two parallel plates (45.7 mm long, 30.5 mm apart).

In the flight tube (ca $5 \cdot 10^{-8}$ mbar, pumped by a 520 L/s turbomolecular pump, Pfeiffer TMU521), a pulsed home-built mass gate is used to mass select ions of interest. The mass gate consists of a stack of parallel shims (thickness 0.5 mm, spaced by 5 mm). They are kept at ±100 V with opposite polarities on adjacent shims and pulsed to ground potential for about 300 ns when the ions under study pass the mass gate, so that the unwanted ions from are removed from the ion beam. Laser irradiation takes place 12 mm behind the mass gate. The photofragments and residual parent ions continue into a two-stage reflectron (Jordan TOF Products), which is used to separate fragments and parents and to analyze the fragment mass. A dual microchannel plate assembly is used to detect the ions.

5. Data acquisition

A photodissociation action spectrum can be obtained by scanning the photon energy and monitoring the yield of photofragments. Trap and mass spectrometer are run at 20 Hz repetition rate while the laser is operated at 10 Hz repetition rate, allowing subtraction of collision induced fragment background from laser induced signal. The laser intensity is measured at the exit window with a Coherent J8LP pyroelectric joulemeter. Every data point is an average of 16 shots, and 5-20 scans were averaged with data taken on different days to ensure reproducibility. The fragment yield Y is calculated according to

$$Y = (I - I_0)\frac{h\nu}{E}, \quad (1)$$

where I and I_0 are the fragment ion signals with and without laser, respectively, E is the laser pulse energy and $h\nu$ is the photon energy. This procedure implicitly assumes that absorption of a single photon leads to fragmentation with unit probability. This may not always be the case, particularly if the photon energy is of the same order as the fragmentation energy threshold or lower. In this case, kinetic shift effects result in suppression of the low-energy side of spectral signatures, and the peak shape of signatures impacted by kinetic shift effects will depend on the trap temperature, which is apparent for $\mathbf{Cu}^+$ and $[\mathbf{Cu}\text{-Cl}]^+$ in the present work.

Mass spectra were recorded on a digital oscilloscope (LeCroy WaveSurfer, 2.5 Gsample/s, 600 MHz), and photodissociation spectra were recorded and normalized by a homebuilt Labview program that reads ion intensity and laser pulse energy from two Tektronix TDS 2022 oscilloscopes (2 Gsample/s, 200 MHz) used to sample data from the MCP detector and a pyroelectric joulemeter (Coherent J8LP).

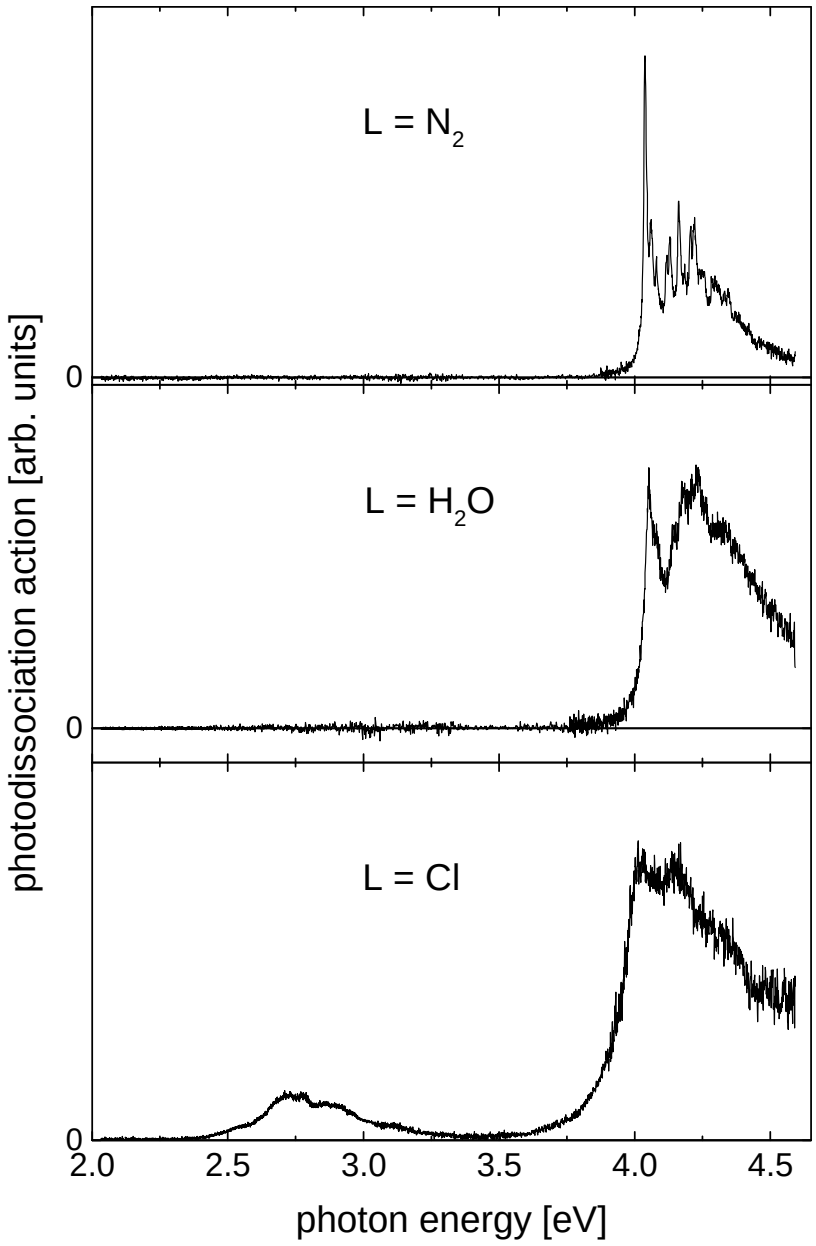

Figure S2. Electronic photodissociation spectra of [**Cu**-L]$^+$ complexes. The photodissociation signal corresponds to the loss of the ligand L in each case. Trap temperatures were 70 K for L = N_2 and 50 K for L = H_2O and Cl.

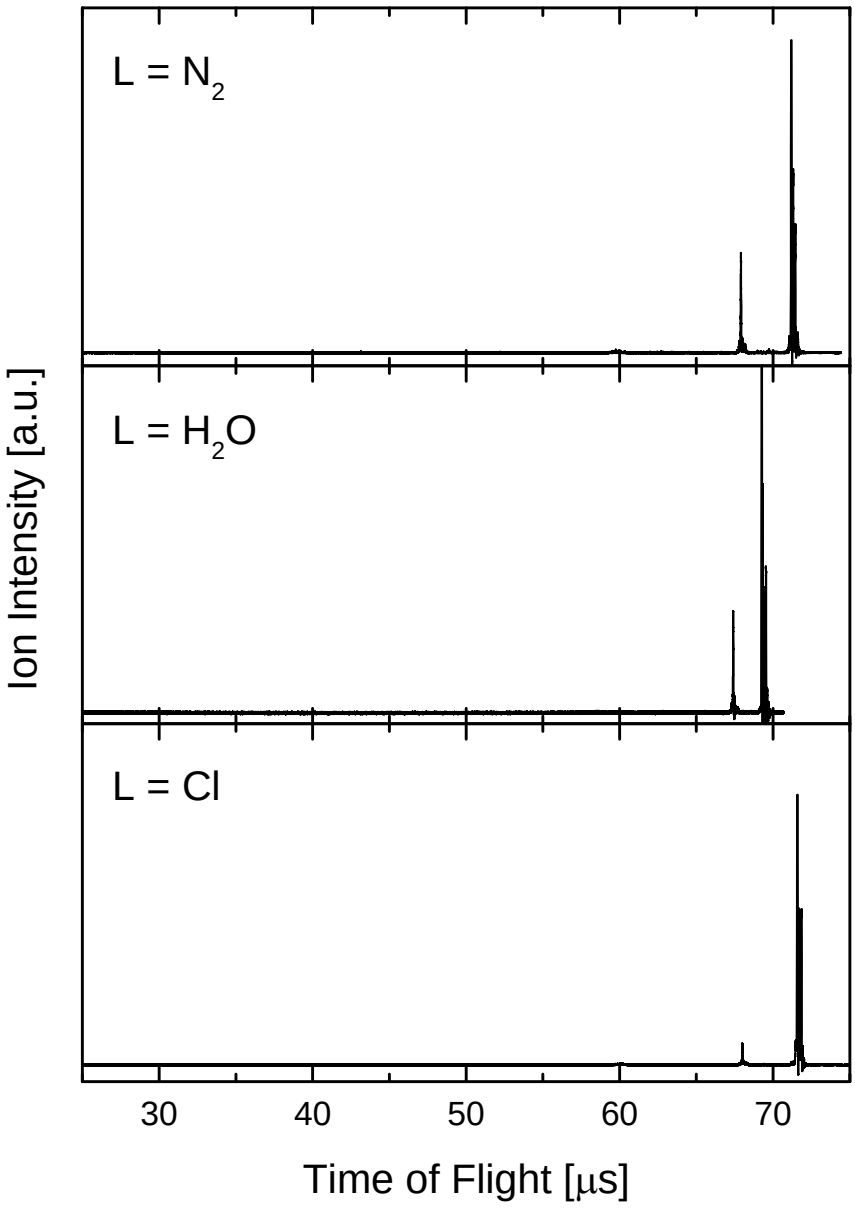

Figure S3. Time-of-flight traces for electronic photodissociation of [**Cu**-L]$^+$ complexes at 4.2 eV photon energy. The ion signal on the right is due to the parent ion, while the smaller peaks are due to the fragment ion signals. Note that only one fragment mass is observed in each case.

Table S1. Calculated totally symmetric vibrational modes of ground state [**Cu**-N_2]$^+$, using PBE0/def2-TZVP (harmonic approximation).

Mode	wavenumber [cm^{-1}]	assignment
13	170	pyridine-Cu-pyridine bend and central C-C stretch
16	240	bipy bend around central C-C bond
17	311	Cu-N_2 stretch
19	381	central C-C stretch
27	673	CNC bending ring deformation
30	783	CCC bending ring deformation
40	1055	CNC bending ring deformation
42	1098	CC stretching ring deformation
44	1143	CH bend
47	1205	CH bend
48	1318	central CC stretch and CN stretching ring deformation
50	1326	central CC stretch and CH bend
52	1363	central CC stretch and CN stretching ring deformation
53	1474	CH bend
56	1538	CH bend and central CC stretch
57	1637	CH bend and ring deformation
59	1661	ring deformation
61	2262	N-N stretch in N_2 ligand
63	3211	CH stretch
65	3218	CH stretch
67	3238	CH stretch
69	3251	CH stretch

Table S2. Calculated totally symmetric vibrational modes of ground state **Cu**$^{+}$, using PBE0/def2-TZVP (harmonic approximation).

Mode	wavenumber [cm^{-1}]	assignment
10	195	pyridine-Cu-pyridine bend and central C-C stretch
13	229	bipy bend around central C-C bond
14	372	central C-C stretch
22	670	CNC bending ring deformation
25	778	CCC bending ring deformation
35	1048	CNC bending ring deformation
37	1099	CC stretching ring deformation
39	1143	CH bend
42	1208	CH bend
43	1314	central CC stretch and CN stretching ring deformation
44	1319	central CC stretch and CH bend
47	1357	central CC stretch and CN stretching ring deformation
48	1472	CH bend
51	1532	CH bend and central CC stretch
52	1636	CH bend and ring deformation
54	1658	ring deformation
57	3210	CH stretch
59	3217	CH stretch
61	3237	CH stretch
63	3257	CH stretch

Table S3. Ground state geometries and nuclear repulsion energies of [**Cu**-L]$^+$ complexes optimized with ωB97X-D/cc-pVTZ.

[**Cu**-N_2]$^+$

Nuclear Repulsion Energy: 1248.9318793625 hartrees

C	-6.5799110	-2.0665366	0.0000000
C	-5.4504468	-4.4218470	0.0000000
C	-2.8382908	-4.5922527	0.0000000
C	-1.4096855	-2.4002697	0.0000000
C	-5.0409652	0.0419360	0.0000000
H	-8.6084605	-1.8570875	0.0000000
H	-6.5820783	-6.1216770	0.0000000
H	-1.9546383	-6.4277244	0.0000000
H	-5.8276573	1.9262666	0.0000000
N	-2.5276987	-0.1191833	0.0000000
C	2.8382908	-4.5922527	0.0000000
C	5.4504468	-4.4218470	0.0000000
C	6.5799110	-2.0665366	0.0000000
C	5.0409652	0.0419360	0.0000000
C	1.4096855	-2.4002697	0.0000000
H	1.9546383	-6.4277244	0.0000000
H	6.5820783	-6.1216770	0.0000000
H	8.6084605	-1.8570875	0.0000000
H	5.8276573	1.9262666	0.0000000
N	2.5276987	-0.1191833	0.0000000
Cu	0.0000000	2.6900637	0.0000000
N	-1.0473141	6.4394129	0.0000000
N	1.0473141	6.4394129	0.0000000

[**Cu**-OH_2]$^+$

Nuclear Repulsion Energy: 1162.5768809371 hartrees

C	-6.5757824	-1.8537475	0.0000000
C	-5.4391495	-4.2055477	0.0000000
C	-2.8283422	-4.3595428	0.0000000
C	-1.4096775	-2.1568293	0.0000000
C	-5.0410191	0.2577251	0.0000000
H	-8.6055614	-1.6540071	0.0000000
H	-6.5620848	-5.9112483	0.0000000
H	-1.9392198	-6.1920463	0.0000000
H	-5.8414766	2.1362637	0.0000000
N	-2.5272320	0.1192964	0.0000000
C	2.8283422	-4.3595428	0.0000000
C	5.4391495	-4.2055477	0.0000000
C	6.5757824	-1.8537475	0.0000000
C	5.0410191	0.2577251	0.0000000
C	1.4096775	-2.1568293	0.0000000
H	1.9392198	-6.1920463	0.0000000
H	6.5620848	-5.9112483	0.0000000
H	8.6055614	-1.6540071	0.0000000
H	5.8414766	2.1362637	0.0000000
N	2.5272320	0.1192964	0.0000000
Cu	0.0000000	3.0248301	0.0000000
O	0.0000000	6.7511783	0.0000000
H	-1.4630983	7.8156796	0.0000000
H	1.4630983	7.8156796	0.0000000

[**Cu**-Cl]$^{+}$

Nuclear Repulsion Energy: 1281.1246689493 hartrees

Cu	0.0000000000	0.0000000000	1.3783264051
C	-3.4655573641	0.0000000000	-1.0326826020
C	-2.9096662433	0.0000000000	-2.2991893211
C	-1.5297734240	0.0000000000	-2.4413198224
C	-0.7399844955	0.0000000000	-1.3085305027
C	-2.6194523261	0.0000000000	0.0596623036
H	-4.5349528056	0.0000000000	-0.8880097756
H	-3.5429317206	0.0000000000	-3.1749376172
H	-1.0881619966	0.0000000000	-3.4254535597
H	-2.9986012535	0.0000000000	1.0719797265
N	-1.2950265722	0.0000000000	-0.0828367450
C	1.5297734240	0.0000000000	-2.4413198224
C	2.9096662433	0.0000000000	-2.2991893211
C	3.4655573641	0.0000000000	-1.0326826020
C	2.6194523261	0.0000000000	0.0596623036
C	0.7399844955	0.0000000000	-1.3085305027
H	1.0881619966	0.0000000000	-3.4254535597
H	3.5429317206	0.0000000000	-3.1749376172
H	4.5349528056	0.0000000000	-0.8880097756
H	2.9986012535	0.0000000000	1.0719797265
N	1.2950265722	0.0000000000	-0.0828367450
Cl	0.0000000000	0.0000000000	3.4406622508